

A quantitative assessment of the accuracy of centroid molecular dynamics for the calculation of the infrared spectrum of liquid water

Francesco Paesani^{1,a)} and Gregory A. Voth²

¹Department of Chemistry and Biochemistry, University of California, San Diego, 9500 Gilman Drive, La Jolla, California 92093, USA

²Department of Chemistry and Center for Biophysical Modeling and Simulation, University of Utah, 315 S. 1400 E. Room 2020, Salt Lake City, Utah 84112-0850, USA

(Received 17 December 2009; accepted 19 December 2009; published online 6 January 2010)

A detailed analysis of the infrared lineshapes corresponding to the intramolecular bond vibrations of HOD in either H₂O or D₂O is presented here in order to quantitatively assess the accuracy of centroid molecular dynamics in reproducing the correct features of the infrared spectrum of water at ambient conditions. Through a direct comparison with the results obtained from mixed quantum-classical calculations, it is shown that centroid molecular dynamics provides accurate vibrational shifts and lineshapes when the intramolecular bond stretching vibrations are described by a physically reasonable anharmonic potential. Artificially large redshifts due to a so-called “curvature problem” are instead obtained with an unphysical shifted harmonic potential because the latter allows substantial probability density at zero bond lengths. © 2010 American Institute of Physics. [doi:10.1063/1.3291212]

I. INTRODUCTION

The exact description of quantum dynamics in the condensed phase remains one of the most challenging problems in theoretical physical chemistry. Since numerical schemes that rely on basis-set expansions or wavepacket propagations scale poorly with the number of degrees of freedom, theoretical approaches based on the path-integral formalism represent an effective alternative for calculating quantum properties in systems with many degrees of freedom. However, due to the associated highly oscillatory behavior, an accurate path integration of the real-time propagators becomes rapidly prohibitive as the time evolves, leading to the well-known “sign problem.” Although a few schemes have been suggested to address this issue,¹ the range of applications of the proposed approaches is still limited.

As a consequence, several approximate methods have been developed in recent years for describing quantum dynamics in condensed phase systems, including centroid molecular dynamics (CMD),^{2–4} semiclassical approaches,⁵ the quantum mode coupling theory,⁶ the Feynman–Kleinert linearized path-integral method,⁷ ring-polymer molecular dynamics (RPMD),⁸ and the effective potential analytic continuation method.⁹ All these methods have been applied with variable degrees of success to the study of several quantum dynamical properties of different condensed phase systems. Besides quantum fluids such as parahydrogen,¹⁰ liquid water is certainly the system that has been most extensively studied through quantum simulations (see Ref. 11 for a recent review). In this regard, it is highly desirable to have access to accurate methodologies for the calculation of the infrared spectrum of water in the OH stretching region, which can

provide detailed information on both the structural and dynamical properties of the liquid phase. This is particularly important in order to achieve a molecular-level understanding of the hydrogen-bond dynamics in terms of the experimental results from ultrafast infrared spectroscopy¹² as well as to test the accuracy of recently developed *ab initio*-based water models.^{13,14} RPMD and CMD have already been applied in combination with the *ab initio*-based TTM3-F force field¹³ to the calculation of the infrared spectrum of liquid water at ambient conditions.^{15,16} The results of Ref. 15 indicate that the infrared spectrum obtained from RPMD simulations is contaminated by the presence of spurious peaks due to unphysical resonances of the internal modes of the imaginary time ring-polymers, while the CMD infrared spectrum has been found to be redshifted (especially in the OH stretching region) relative to the experimental data,^{15,16} which has been attributed to some inaccuracies of the TTM3-F water model.¹⁶ By contrast, it has recently been shown that the CMD infrared spectrum computed for an isolated water molecule in the gas phase having a shifted harmonic bond stretching potential suffers by a so-called “curvature problem,” which leads to artificially redshifted and broad lineshapes for that potential.¹⁷ As described in detail in Ref. 17, within a path-integral representation and assuming an “asymptotic approximation” for the OH bond in the limit of infinite oxygen mass and infinitely stiff harmonic constant, the “quasiparticles” or “beads” of the ring-polymer that define the hydrogen atom always move on the surface of a sphere with radius $R > 0$. However, since the centroid coordinates are defined as the centers of mass of the corresponding path-integral ring-polymers, it is thus possible that the centroid position of the H atom can also (unphysically) reside inside the sphere. This causes the centroid dynamics to be influenced by unphysical “curvature” and hence leads to the above mentioned problems for the infrared lineshape.

^{a)}Author to whom correspondence should be addressed. Electronic mail: fpaesani@ucsd.edu.

The curvature problem is accentuated in the shifted harmonic oscillator because it has nonzero probability density for unphysical values of $R=0$ (i.e., the potential is finite there). A more physically realistic OH stretching potential that prevents the actual bond length (R) from being shorter than the distance determined by the physical repulsive “wall” (R_{wall}) would therefore be expected to have less of a curvature problem in CMD simulations. Either way, the curvature problem is expected to be more pronounced at low temperature and/or for more quantum-mechanical vibrations because, in these cases, the path-integral ring-polymers are more extended and, consequently, the centroid bond length may become appreciably shorter than R_{wall} .

The objective of this study is to investigate the occurrence of the curvature problem and to quantitatively assess its effects in CMD simulations of the infrared lineshapes corresponding to the intramolecular stretching vibrations of liquid water at ambient conditions. The focus here is especially on the nature of this issue when a realistic anharmonic OH bond stretching potential is employed which has a more repulsive behavior at short OH distances and a softer behavior at OH distances beyond the equilibrium value.

II. COMPUTATIONAL METHODOLOGIES

The present analysis of the infrared lineshapes for the stretching vibrations in liquid water is carried out for two systems consisting of a single HOD molecule with either 127 H₂O or D₂O molecules (which hereafter will be referred to as the HOD:H₂O and HOD:D₂O systems, respectively) contained in a periodic cubic box. In all calculations, the water interactions were described by the point charge and flexible qSPC/Fw model¹⁸ with the long-range electrostatic interactions being treated according to the Ewald method.¹⁹ Following Ref. 20, a modified version of the qSPC/Fw model was also employed in which the original harmonic potential used to describe the intramolecular stretching motion was replaced by a more physically realistic quartic approximation to a Morse potential

$$V(R) = D \left[\alpha^2 (R - R_{\text{eq}})^2 - \alpha^3 (R - R_{\text{eq}})^3 + \frac{7}{12} \alpha^4 (R - R_{\text{eq}})^4 \right]. \quad (1)$$

In Eq. (1), the parameters $D=116.09$ kcal mol⁻¹ and $\alpha = 2.287$ Å⁻¹ were taken from Ref. 20, R defines the OD (OH) stretching coordinate with R_{eq} being set to 1.0 Å as in the original qSPC/Fw model.¹⁸ In the following, these two water models will be referred to as the “harmonic qSPC/Fw” and “anharmonic qSPC/Fw” models, respectively. It is important to emphasize that in the simulations described here, the anharmonic functional form adopted for the intramolecular stretching vibrations was not specifically designed for accurately reproducing the corresponding vibrational bands in liquid water. Instead, such an anharmonic potential only provides a convenient and more realistic description of the intramolecular stretching motion of the water molecules in the condensed phase relative to a more simplified description that is obtained with a shifted harmonic bond stretching po-

tential. The latter potential lacks a “steep wall” as $R \rightarrow 0$ so that significant probability density can accumulate in this model at small unphysical values of R .

The initial classical equilibrium configurations were obtained from classical molecular dynamics (MD) runs for a total of 1 ns for a system consisting of 128 H₂O molecules which were performed at ambient conditions ($T=300$ K and $P=1$ atm) with temperature and pressure maintained via Langevin dynamics and Berendsen barostat,¹⁹ respectively. The path-integral molecular dynamics method in the normal mode representation (NMPIMD) (Ref. 21) was then used to perform two NPT simulations of 500 ps each for both the HOD:H₂O and HOD:D₂O systems in order to obtain the corresponding quantum-mechanical equilibrium configurations. In the NMPIMD simulations the quantum partition function was discretized with 32 quasiparticles or beads,²¹ while the propagation was performed with a timestep $\Delta t = 0.2$ fs. The temperature was controlled via Nosé–Hoover chains (NHC) of four thermostats²² that were coupled to each path-integral normal mode. The isothermal-isobaric ensemble was generated according to the algorithm illustrated in Ref. 23.

Starting from the corresponding equilibrated configurations, 100 independent classical trajectories of 25 ps each in the NVE ensemble were simulated for both the HOD:H₂O and HOD:D₂O systems at $T=300$ K. The infrared lineshapes for the OH and OD stretching vibrations of the HOD molecule were calculated according to the following well-known expression²⁴

$$I(\omega) \approx \int_{-\infty}^{+\infty} dt e^{-i\omega t} \langle \mu(0) \cdot \mu(t) \rangle, \quad (2)$$

where $\langle \mu(0) \cdot \mu(t) \rangle$ is the HOD dipole autocorrelation function computed from the classical trajectories. The corresponding quantum dynamical simulations were performed using CMD with the centroid forces computed “on the fly” according to the adiabatic time scale separation scheme (ACMD scheme).^{2(c)} Starting from the equilibrated NMPIMD molecular configurations, 50 independent ACMD trajectories of 25 ps each were simulated. The ACMD propagation of the centroid degrees of freedom was carried out in the NVE ensemble with NHC of four thermostats attached to each nonzero frequency normal mode. An adiabaticity parameter^{2(c)} $\gamma=0.5$ and a time step $\Delta t=0.05$ fs were used, and the dipole autocorrelation function in Eq. (2) was calculated within a classical representation of the dipole operator.³

In order to quantitatively assess the accuracy of CMD in reproducing the OD (OH) vibrational shift in HOD in the HOD:H₂O (HOD:D₂O) system, the corresponding infrared lineshape was also computed according to a well-established mixed quantum-classical (QC) scheme.²⁵ This approach provides a very accurate approximation to the actual infrared lineshape when a well defined vibrational mode of a dilute chromophore exists, as in the present case of the OH (OD) vibration of a single HOD molecule in D₂O (H₂O). As described in detail in Ref. 26, within the QC scheme the OD

(OH) spectral line, $I^{QC}(\omega)$, corresponding to the 1–0 vibrational transition of the HOD molecule in H_2O (D_2O) can be expressed as

$$I^{qc}(\omega) \approx \int_{-\infty}^{+\infty} dt e^{-i\omega t} \left\langle \mu_{10}(0) \cdot \mu_{10}(t) \right. \\ \left. \times \exp \left[i \int_0^t d\tau \omega_{10}(\tau) \right] \right\rangle, \quad (3)$$

where $\mu_{10}(t)$ and $\omega_{10}(t)$ are, respectively, the vibrational transition moment and the vibrational frequency associated to the transition between the ground and excited state of the OD (OH) stretch at time t , and the brackets denote a classical equilibrium average. Equation (3) should also contain an additional factor dependent on the lifetime of the vibrational excited state which, however, for the purposes of the present study can be safely neglected. The OD (OH) frequencies were computed for all the HOD: H_2O (HOD: D_2O) molecular configurations extracted from either classical MD or ACMD trajectories by solving the Schrödinger equation for the corresponding one-dimensional (1D) OD (OH) oscillator using the Numerov method.²⁷ Following the procedure described in Ref. 28, for any given configuration of the HOD: H_2O (HOD: D_2O) system, the underlying OD (OH) Born–Oppenheimer potential energy curve was computed by stretching the OD (OH) bond while keeping the positions of all other atoms fixed. The resulting potential curve was then used to compute the corresponding vibrational frequency as well as the vibrational wave functions of the ground and first excited states. The vibrational transition moments $\mu_{10}(t)$, were calculated within the same computational scheme from the numerical integration over the product of the molecular dipole moment and the appropriate vibrational wave functions. In solving the 1D Schrödinger equation, all the molecular interactions were consistently described by either the harmonic qSPC/Fw or the anharmonic qSPC/Fw model. It is important to note that, even in the case where the molecular configurations were extracted from the ACMD trajectories, the centroid coordinates were simply utilized to define the instantaneous positions of all atoms at time t , which were then used to determine the underlying Born–Oppenheimer potential energy curve. The latter is not to be confused with the effective centroid potential that instead determines the actual centroid dynamics in a direct ACMD simulation.⁴ An identical approach has already been applied in Ref. 16 to the study of the OD (OH) infrared lineshapes of HOD in H_2O (D_2O) with the TTM3-F water model.

III. RESULTS AND DISCUSSION

A. Harmonic qSPC/Fw model

The OD infrared lineshapes $I(\omega)$ of the HOD molecule in H_2O calculated according to Eq. (2) from both classical (panel a) and ACMD (panel c) simulations with the harmonic qSPC/Fw model are compared in Fig. 1 with the corresponding quantum-mixed lineshapes, $I^{QC}(\omega)$ of Eq. (3), shown in panels b and d, respectively. Also shown in panels b and d are the corresponding static frequency distributions $P(\omega)$ obtained from binning the instantaneous OD frequencies calcu-

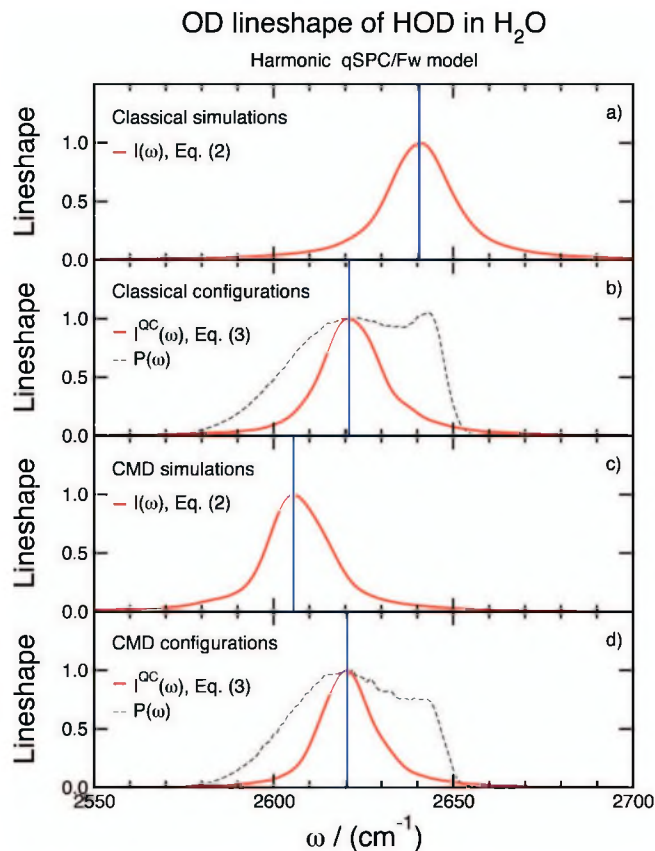


FIG. 1. OD lineshape of HOD in H_2O computed with the harmonic qSPC/Fw model at $T=300$ K. Panel a: Classical lineshape calculated via Eq. (2) using classical MD simulations. Panel b: Mixed QC lineshape calculated via Eq. (3) using molecular configurations extracted from classical MD simulations. Panel c: CMD lineshape calculated via Eq. (2) using ACMD simulations. Panel d: Mixed QC lineshape calculated via Eq. (3) using molecular configurations extracted from ACMD simulations.

lated according to the procedure illustrated in Sec. II from the 1D Schrödinger equation for the OD stretching vibration of the HOD molecule. An analogous comparison is reported in Fig. 2 for the OH infrared lineshape of the HOD molecule in D_2O . In both figures, the solid blue lines identify the peak position of each spectral line.

The two sets of results in Figs. 1 and 2 provide qualitatively similar information. First of all, it is important to note that the mixed QC lineshapes obtained from both classical and ACMD configurations are in excellent agreement with each other, which is due to the similarity between classical and quantum structural properties of liquid water at ambient conditions (e.g., see Ref. 29). It is also apparent that both the OD and OH classical spectral lines display a similar shape as the corresponding $I^{QC}(\omega)$ although they are consistently blueshifted by about 1%. As already noted in previous classical simulations with empirical force fields, the static frequency distributions are instead much broader than the corresponding $I^{QC}(\omega)$.³⁰ In addition, both $P(\omega)$ show a shoulder on the blue side of the band, which is somewhat more pronounced in the curves obtained from molecular configurations that are extracted from classical simulations. Interestingly, these shoulders appear at the same frequencies as the corresponding classical spectral lines. This correspondence can be explained by considering that the blue side of the OD

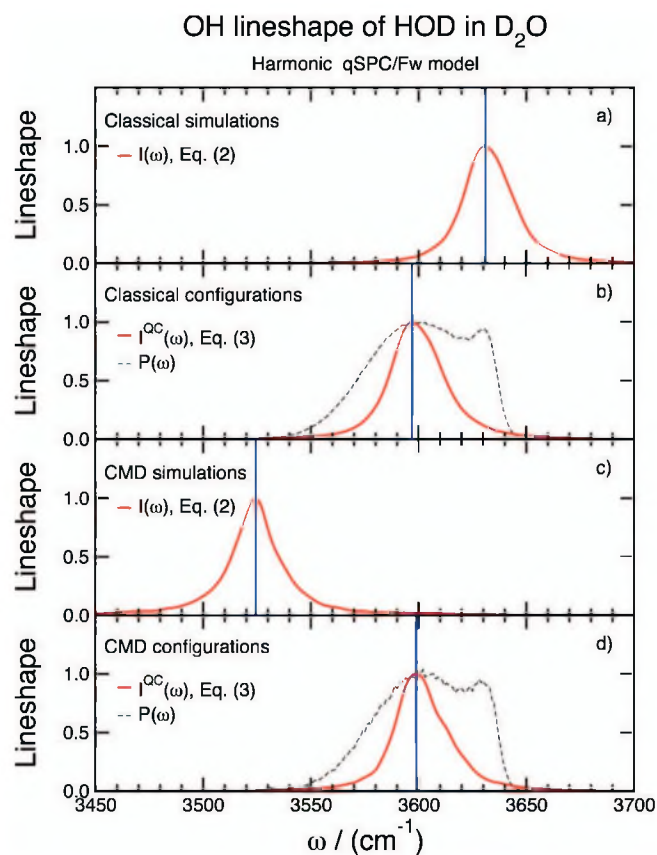


FIG. 2. OD lineshape of HOD in D_2O computed with the harmonic qSPC/Fw model at $T=300$ K. Panel a: Classical lineshape calculated via Eq. (2) using classical MD simulations. Panel b: Mixed QC lineshape calculated via Eq. (3) using molecular configurations extracted from classical MD simulations. Panel c: CMD lineshape calculated via Eq. (2) using ACMD simulations. Panel d: Mixed QC lineshape calculated via Eq. (3) using molecular configurations extracted from ACMD simulations.

(OH) infrared lineshape is due to adsorption by the most weakly hydrogen-bonded configurations in which, consequently, the HOD molecule interact more weakly with the surrounding molecules. For these configurations, the anharmonic effects that arise from the coupling of the (harmonic) intramolecular motion with the environment are thus significantly reduced. Therefore, being essentially determined by the intramolecular potential represented by the harmonic qSPC/Fw model, the potential energy surface corresponding to the most weakly hydrogen-bonded molecular configurations is thus effectively harmonic, for which classical simulations provide the correct vibrational frequencies.

Based on the comparison with the corresponding mixed QC lineshapes, it is also possible to quantitatively assess the accuracy of CMD in reproducing the vibrational shift in the OD (OH) stretch of the HOD molecule in H_2O (D_2O) with a harmonic representation of the intramolecular motion. Figures 1 and 2 clearly show that the ACMD lineshapes are consistently redshifted relative to $I^{QC}(\omega)$. Importantly, this redshift (contrary to the blueshift displayed by the classical lineshapes) is appreciably different for the OD and OH vibrations of HOD, going from less than 1% for the OD stretch to almost 2% for the OH stretch relative to the position of the corresponding mixed QC lineshapes. This is a clear manifestation of the curvature problem that affects CMD simulations

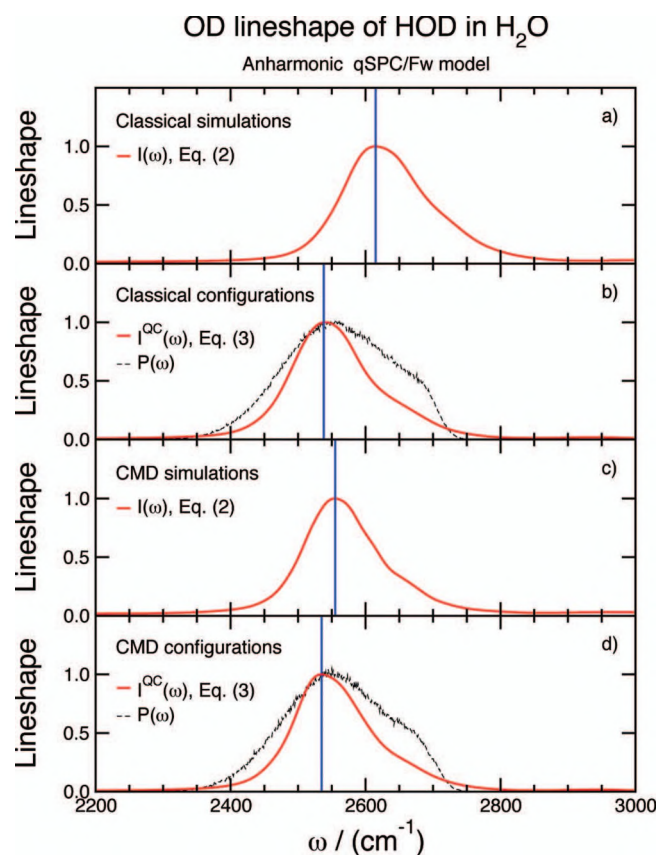


FIG. 3. OD lineshape of HOD in H_2O computed with the anharmonic qSPC/Fw model at $T=300$ K. Panel a: Classical lineshape calculated via Eq. (2) using classical MD simulations. Panel b: Mixed QC lineshape calculated via Eq. (3) using molecular configurations extracted from classical MD simulations. Panel c: CMD lineshape calculated via Eq. (2) using ACMD simulations. Panel d: Mixed QC lineshape calculated via Eq. (3) using molecular configurations extracted from ACMD simulations.

in Cartesian coordinates leading to artificially redshifted and broader lineshapes.¹⁷ As mentioned above, this effect is more pronounced at low temperature and/or for more quantum-mechanical vibrations, which explains the larger magnitude of the redshift predicted by the ACMD simulations for the OH stretch relative to that obtained for the OD stretch. However, it is important to reiterate that because of the lack of a physically correct repulsive wall at short distance, a purely harmonic potential leads to an unphysical description of the molecular stretching motion. The CMD simulations are clearly influenced by this unphysical behavior of the potential energy function.

B. Anharmonic qSPC/Fw model

In order to quantitatively assess the effects of the curvature problem in CMD simulations of the infrared spectrum of liquid water at ambient conditions with a more realistic description of the molecular interactions, the analysis of Sec. III A was also repeated using the anharmonic qSPC/Fw model. The infrared lineshapes obtained from classical and ACMD simulations of both HOD: H_2O and HOD: D_2O systems are shown in Figs. 3 and 4, respectively. As in the case with the harmonic qSPC/Fw model, the mixed QC lineshapes obtained from classical and ACMD configurations

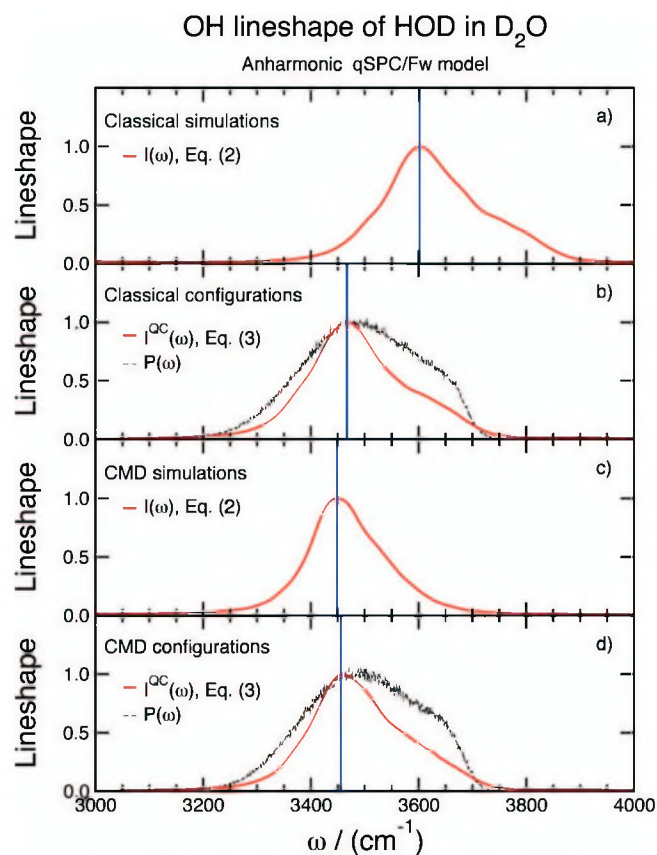


FIG. 4. OH lineshape of HOD in D₂O computed with the anharmonic qSPC/Fw model at T=300 K. Panel a: Classical lineshape calculated via Eq. (2) using classical MD simulations. Panel b: Mixed QC lineshape calculated via Eq. (3) using molecular configurations extracted from classical MD simulations. Panel c: CMD lineshape calculated via Eq. (2) using ACMD simulations. Panel d: Mixed QC lineshape calculated via Eq. (3) using molecular configurations extracted from ACMD simulations.

(panels b and d) are in excellent agreement with each other, which again results from the close similarity between the underlying classical and ACMD structural arrangement of liquid water.²⁹ The corresponding static frequency distributions are broader and show slightly less pronounced shoulders on the blue side relative to those observed in Figs. 1 and 2 for the $P(\omega)$ obtained with the harmonic qSPC/Fw model. Similar differences between the $P(\omega)$ and $I^{QC}(\omega)$ lineshapes have already been observed in classical simulations with the SPC/E water model combined with electronic structure calculations.³⁰ It is interesting to note that somewhat less pronounced differences have been found in a similar analysis carried out with the *ab initio*-based TTM3-F water model,¹⁶ which suggests that the magnitude of the dynamical effects on the OD (OH) infrared lineshape is particularly sensitive to the model employed to describe the intramolecular motion as well as on the local arrangement of the water molecules predicted by a specific simulation approach.

Similar to the results discussed in Sec. III A, the OD and OH infrared lineshapes calculated from the corresponding classical dipole autocorrelation functions (panels a of Figs. 3 and 4, respectively) are blueshifted relative to the mixed QC lineshapes. However, clearly contrary to the results of Sec. III A with the harmonic qSPC/Fw model, the blueshift in the classical lineshapes relative to $I^{QC}(\omega)$, which is obtained

with the anharmonic qSPC/Fw model, is noticeably different between the OD (~2%) and OH (~4%) stretching vibrations. This can be explained by considering that, as discussed above, the OH stretch is significantly more quantum-mechanical than the OD stretch and, consequently, the effects of the anharmonicity (which are not captured by classical simulations) are significantly larger.

Based on the comparison reported in Figs. 3 and 4, the present analysis of the OH and OD lineshapes of a single HOD molecule in H₂O and D₂O thus allows for a quantitative assessment of the accuracy of CMD in reproducing the infrared spectrum of liquid water at ambient conditions. The results shown in panels c of both figures clearly indicate that the ACMD infrared lineshapes are in very close agreement with the corresponding mixed QC lineshapes. Such level of agreement demonstrates that ACMD simulations carried out with a more physical representation of the intramolecular motion reproduce the correct redshift for both the OD and OH stretching vibrations of HOD in the liquid phase at ambient conditions. Some evidence for a similar behavior have already been presented in Ref. 16 for ACMD simulations of the infrared spectra of water calculated with the *ab initio*-based TTM3-F model and in an earlier work.³¹ The present analysis thus suggests that, although the curvature problem is intrinsic to the CMD method, its effects appear to be negligible for the calculation of the infrared spectrum of liquid water at ambient conditions when the intramolecular vibrational motion is represented in a physical fashion.

IV. CONCLUSIONS

In this study a detailed analysis of the OD and OH infrared lineshapes of a single HOD molecule in either H₂O or D₂O at ambient conditions has been carried out, employing classical and CMD simulations as well as a mixed QC approach. Use of both harmonic and anharmonic potentials to describe the intramolecular bond vibrations of the water molecules has allowed for a quantitative assessment of the accuracy of CMD in reproducing the infrared lineshapes of both the OD and OH stretching vibrations of HOD in the liquid phase. The results of this study provide quantitative evidence that the curvature problem affects the position of the spectral lines obtained from CMD simulations with a shifted and unphysical harmonic description of the intramolecular motion, which leads to artificially large redshifts relative to the corresponding lineshapes calculated within a mixed QC approach. By contrast, when the intramolecular motion is described by a more realistic anharmonic potential, the analysis presented here clearly demonstrates that CMD is capable to capture the correct redshift for both the OD and OH stretching vibrations at ambient conditions, providing very close agreement with the corresponding mixed QC lineshapes. A thorough investigation of the effects of the curvature problem in CMD simulations of the infrared spectrum of liquid water under different conditions with a more physical description of the molecular interactions in terms of the *ab initio*-based TTM3-F force field, as well as a direct comparison between CMD and semiclassical approaches, will be the subject of two forthcoming publications.³²

ACKNOWLEDGMENTS

This research was supported in part by the Office of Naval Research through Grant No. N00014-05-1-0457.

- ¹C. H. Mak and D. Chandler, *Phys. Rev. A* **44**, 2352 (1991); M. Topaler and N. Makri, *J. Chem. Phys.* **97**, 9001 (1992).
- ²(a) J. Cao and G. A. Voth, *J. Chem. Phys.* **100**, 5093 (1994); (b) **101**, 6157 (1994); (c) **101**, 6168 (1994); (d) **101**, 6184 (1994).
- ³J. Cao and G. A. Voth, *J. Chem. Phys.* **100**, 5106 (1994).
- ⁴S. Jang and G. A. Voth, *J. Chem. Phys.* **111**, 2357 (1999); **111**, 2371 (1999).
- ⁵W. H. Miller, *J. Phys. Chem. A* **105**, 2942 (2001); N. Makri, *ibid.* **108**, 806 (2004).
- ⁶D. R. Reichman and E. Rabani, *Phys. Rev. Lett.* **87**, 265702 (2001).
- ⁷J. A. Poulsen, G. Nyman, and P. J. Rossky, *J. Chem. Phys.* **119**, 12179 (2003).
- ⁸I. R. Craig and D. E. Manolopoulos, *J. Chem. Phys.* **121**, 3368 (2004).
- ⁹A. Horikoshi and K. Kinugawa, *J. Chem. Phys.* **119**, 4629 (2003).
- ¹⁰T. D. Hone and G. A. Voth, *J. Chem. Phys.* **121**, 6412 (2004); J. Liu and W. H. Miller, *ibid.* **128**, 144511 (2008); T. F. Miller III and D. E. Manolopoulos, *ibid.* **122**, 184503 (2005); A. Nakayama and N. Makri, *ibid.* **119**, 8592 (2003); E. Rabani, D. R. Reichman, G. Krilov, and B. J. Berne, *Proc. Natl. Acad. Sci. U.S.A.* **99**, 1129 (2002).
- ¹¹F. Paesani and G. A. Voth, *J. Phys. Chem. B* **113**, 5702 (2009).
- ¹²H. J. Bakker and J. L. Skinner, *Chem. Rev.* (2009) doi:10.1021/cr9001879.
- ¹³G. S. Fanourgakis and S. S. Xantheas, *J. Chem. Phys.* **128**, 074506 (2008).
- ¹⁴W. Cencek, K. Szalewicz, C. Leforestier, R. van Harrevelt, and A. van der Avoird, *Phys. Chem. Chem. Phys.* **10**, 4716 (2008); Y. Wang, B. C. Shepler, B. J. Braams, and J. M. Bowman, *J. Chem. Phys.* **131**, 054511 (2009).
- ¹⁵S. Habershon, G. S. Fanourgakis, and D. E. Manolopoulos, *J. Chem. Phys.* **129**, 074501 (2008).
- ¹⁶F. Paesani, S. S. Xantheas, and G. A. Voth, *J. Phys. Chem. B* **113**, 13118 (2009).
- ¹⁷A. Witt, S. D. Ivanov, M. Shiga, H. Forbert, and D. Marx, *J. Chem. Phys.* **130**, 194510 (2009).
- ¹⁸F. Paesani, W. Zhang, D. A. Case, T. E. Cheatham III, and G. A. Voth, *J. Chem. Phys.* **125**, 184507 (2006).
- ¹⁹D. Frenkel and B. Smit, *Understanding Molecular Simulation: From Algorithms to Applications* (Academic Press, New York, 2001).
- ²⁰S. Habershon, T. E. Markland, and D. E. Manolopoulos, *J. Chem. Phys.* **131**, 024501 (2009).
- ²¹B. J. Berne and D. Thirumalai, *Annu. Rev. Phys. Chem.* **37**, 401 (1986).
- ²²G. J. Martyna, M. L. Klein, and M. Tuckerman, *J. Chem. Phys.* **97**, 2635 (1992).
- ²³G. J. Martyna, A. Hughes, and M. E. Tuckerman, *J. Chem. Phys.* **110**, 3275 (1999).
- ²⁴R. Zwanzig, *Nonequilibrium Statistical Mechanics* (Oxford University Press, Oxford, 2001).
- ²⁵S. Mukamel, *Principles of Nonlinear Optical Spectroscopy* (Oxford University Press, New York, 1995).
- ²⁶J. L. Skinner, *Mol. Phys.* **106**, 2245 (2008).
- ²⁷B. V. Numerov, *Mon. Not. R. Astron. Soc.* **84**, 592 (1924).
- ²⁸E. Harder, J. D. Eaves, A. Tokmakoff, and B. J. Berne, *Proc. Natl. Acad. Sci. U.S.A.* **102**, 11611 (2005).
- ²⁹F. Paesani, S. Iuchi, and G. A. Voth, *J. Chem. Phys.* **127**, 074506 (2007).
- ³⁰J. R. Schmidt, S. T. Roberts, J. J. Loparo, A. Tokmakoff, M. D. Fayer, and J. L. Skinner, *Chem. Phys.* **341**, 143 (2007).
- ³¹G. K. Schenter, B. C. Garrett, and G. A. Voth, *J. Chem. Phys.* **113**, 5171 (2000).
- ³²F. Paesani (unpublished).